

Time-domain and spectral-domain investigation of inflection-point slow-light modes in photonic crystal coupled waveguides

Shih-Chieh Huang^{1,2}, Masao Kato^{2*}, Eiichi Kuramochi^{2*}, Chien-Ping Lee¹, and Masaya Notomi^{2*}

¹ Department of Electronics Engineering, National Chiao Tung University, Hsinchu 300, Taiwan

² NTT Basic Research Labs, NTT Corporation, 3-1 Morinosato-Wakamiya, Atsugi, 243-0198, Japan

* also at CREST-JST, 4-1-8 Honmachi, Kawaguchi, Saitama 332-0012, Japan

schuang.ee91g@nctu.edu.tw

Abstract: We report on spectral-domain and time-domain measurements and numerical calculations of group velocities in a photonic crystal coupled waveguide, where the unique guided mode band structure has a flat band region within the photonic band gap allowing for slow light observation. The spectral dependence of group velocity, which is measured by interference method, indicates the existence of slow light modes around the inflection point of the unique flat band, rather than at the band edge. Time-domain observation of optical pulses propagating along two-dimension slab photonic crystal coupled waveguides is also demonstrated by using a high speed oscilloscope. By adjusting the wavelength of the input pulses toward the flat band of the coupled defect modes, an increasing duration time between reference and output pulses are clearly observed. An extremely small group velocity of $0.017c$ is thus obtained. Calculated group velocities show good agreement with our measured results.

©2007 Optical Society of America

OCIS codes: (230.7370) Waveguides; (250.5300) Photonic integrated circuits; (999.9999) Slow light.

References and links

1. D. Mori and T. Baba, "Dispersion-controlled optical group delay device by chirped photonic crystal waveguides," *Appl. Phys. Lett.* **85**, 1101 (2004).
2. M. L. Povinelli, S. G. Johnson, and J. D. Joannopoulos, "Slow-light, band-edge waveguides for tunable time delays," *Opt. Express* **13**, 7145 (2005).
3. A. Yariv, Y. Xu, R. K. Lee, and A. Sherer, "Coupled-resonator optical waveguide: a proposal and analysis," *Opt. Lett.* **24**, 711 (1999).
4. T. J. Karle, D. H. Brown, R. Wilson, M. Steer, and T. F. Krauss, "Planar photonic crystal coupled cavity waveguides," *IEEE J. Select. Tops. Quantum Electron.* **8**, 909 (2002).
5. M. F. Yanik, W. Suh, Z. Wang, and S. Fan, "Stopping light in a waveguide with an all-optical analog of electromagnetically induced transparency," *Phys. Rev. Lett.* **93**, 233903 (2004).
6. M. Notomi, K. Yamada, A. Shinya, J. Takahashi, C. Takahashi, and I. Ypkoama, "Extremely large group-velocity-dispersion of line-defect waveguides in photonic crystal slabs," *Phys Rev. Lett.* **87**, 253902 (2001).
7. A. Y. Petrov and M. Eich, "Zero dispersion at small group velocities in photonic crystal waveguides," *Appl. Phys. Lett.* **85**, 4866 (2004).
8. Y. A. Vlasov, M. O'Boyle, H. F. Hamann, and S. J. McNab, "Active control of slow light on a chip with photonic crystal waveguides," *Nature* **438**, 65 (2005).
9. R. S. Jacoben, A. V. Lavrinenko, L. H. Frandsen, C. Peucheret, B. Zsigri, G. Moulin, J. F. Pedersen, and P. I. Borel, "Direct experimental and numerical determination of extremely high group indices in photonic crystal waveguides," *Opt. Express* **13**, 7861 (2005).
10. J. Huang, C. M. Reinke, A. Jafarpour, B. Momeni, M. Soltani, and Ali Adibi, "Observation of large parity change-induced dispersion in triangular-lattice photonic crystal waveguides using phase sensitive techniques," *Appl. Phys. Lett.* **88**, 071111 (2006).
11. T. Asano, K. Kiyota, D. Kumamoto, B. S. Song, and S. Noda, "Time-Domain measurement of pico-second light propagation in a two-dimensional photonic crystal slab waveguide," *Appl. Phys. Lett.* **84**, 4690 (2004).

12. H. Gersen, T. J. Karle, R. J. P. Engelen, W. Bogaerts, J. P. Korterik, N. F. van Hulst, T. F. Krauss, and L. Kuipers, "Real-space observation of ultraslow light in photonic crystal waveguides," *Phys Rev. Lett.* **94**, 073903 (2005).
 13. D. Mori and T. Baba, "Wideband and low dispersion slow light by chirped photonic crystal coupled waveguide," *Opt. Express* **13**, 9398 (2005).
 14. N. Yamamoto, T. Ogawa, and K. Komori, "Photonic crystal directional coupler switch with small switching length and wide band width," *Opt. Express* **14**, 1223 (2006).
 15. Y. A. Vlasov and S. J. McNab, "Coupling into the slow light mode in slab-type photonic crystal waveguides," *Opt. Lett.* **31**, 50 (2006).
-

1. Introduction

Utilizing photonic band gap structures to slow down the speed of light has recently been acquiring much attention because of potential applications in devices such as optical delay lines [1, 2], all-optical buffers [3, 4], and optical storages [5]. One such promising structure is two-dimensional (2D) photonic crystal (PhC) slab waveguides [6]. If properly designed, these waveguides exhibit a unique dispersion relationship for the traveling light and can selectively retard the propagation speed of certain waveguide modes. Theoretical calculations have shown that extremely small group velocities can exist for the defect mode at the band edge of PhC waveguides due to a relatively flat band structure [6, 7]. Experimental measurements of slow light in PhC waveguides have also been reported. Some used the frequency-domain approach, which indirectly deduce the group index by analyzing the transmission spectrum using Fabry-Perot or interference methods [6, 8]. Some measured the phase delay of modulated signal to determine the group velocities [9, 10]. Results from direct time-domain measurements on the wave propagation in PhC waveguides, however, are very limited [11, 12] because of the narrow operation bandwidth and large group-velocity-dispersion at the band edge.

Recently, Mori and Baba proposed a photonic crystal coupled waveguide (PhCCW), where a unique flat band of coupled modes is formed in the photonic band gap [13]. An S-shaped dispersion curve with a flat region (or the inflection point) inside the first Brillouin zone was obtained for the waveguide mode. Their simulation results showed that the waveguide mode has a wider operation bandwidth and a lower dispersion for slow light propagation than that of a conventional single line-defect PhC waveguide. However, the experimental realization of a PhCCW and the light behavior at the unique flat band have not been reported.

In this paper, we present for the first time the measured transmission spectrum of a properly designed PhCCW to verify the existence of the unique flat band. Next, we demonstrate the deduced group velocities as a function of wavelengths by using an interference approach, where the spectra of an integrated Mach-Zehnder interferometer (MZI) employing PhCCWs were measured, to further clarify the inflection-point slow light modes of this flat region. Finally, we report the time-domain observation of the retardation of propagation pulses in a 2D slab PhCCW by using a high speed oscilloscope. The group velocities of the optical pulses at different wavelengths were measured. An extremely small group velocity of $0.017c$ was obtained at the wavelength of $\lambda = 1537.30$ nm, which is very close to the inflection-point slow light modes in the flat band.

2. Device design and fabrication

A PhCCW consists of two W1 type waveguides, where a row of air-holes (W1) is removed from the otherwise hexagonal PhC lattices [14]. The two W1 waveguides are separated by three rows of air holes. The radius of the holes in the center row and those besides the waveguides and the position of the holes along the W1 waveguides are used as design parameters. We fabricated the coupled waveguide structures on a 4-inch silicon-on-insulator (SOI) wafer with a $3\ \mu\text{m}$ buried oxide layer and a thin silicon guiding layer (thickness = 205 nm). The photonic crystal with hexagonal lattices having lattice constant $a = 438\text{nm}$ was defined by E-beam lithography. The air holes were obtained by etching through the silicon

layer using an inductively coupled plasma reactive ion etcher (ICP-RIE). After etching the silicon layer, the suspended silicon membrane was formed by removing the buried oxide layer using a selective wet etch, an HF solution. The top view of a completed coupled waveguide is shown in Fig. 1(a).

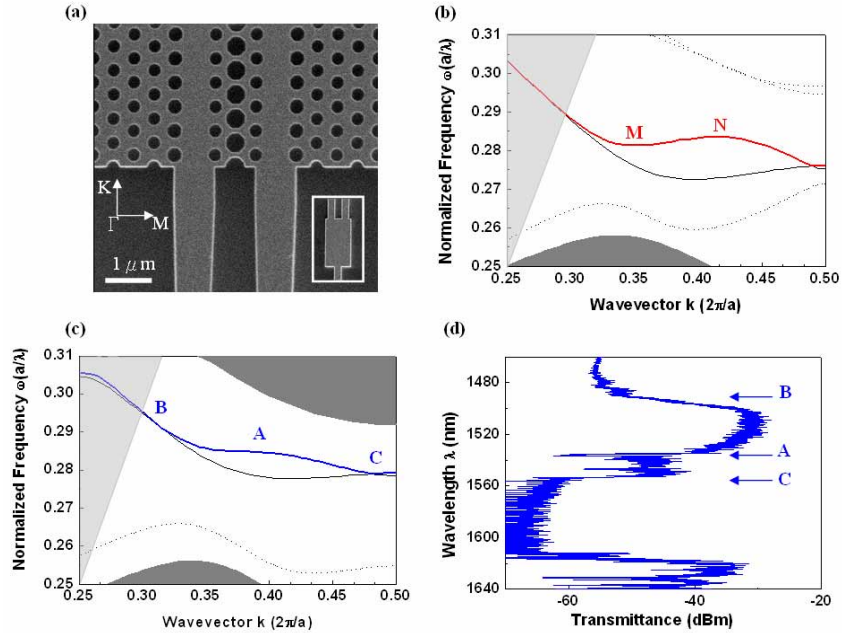


Fig. 1. (a). SEM image of PhCCW with lattice constant $a = 438$ nm and hole diameter $2r_0=250$ nm. The radius of holes in the center row (r_c) and those besides the waveguides (r_1, r_2) are designed as $r_c=0.44a$, $r_1=0.23a$, and $r_2=0.30a$, respectively. The position of holes with radius r_2 shifted toward the waveguides (s_2) is $0.15a$. The inset shows MMI devices with dimension $3.2 \mu\text{m} \times 5.7 \mu\text{m}$ used in the experiments. (b) and (c) are the calculated band diagrams of PhCCWs with different structural parameters: $(r_0, r_c, r_1, r_2, s_2) = (0.30a, 0.44a, 0.30a, 0.33a, 0.00a)$ in (b) and $(0.28a, 0.41a, 0.26a, 0.27a, 0.22a)$ in (c). The black line and S-shape-like of blue (or red) line represent the odd and even modes of coupled bands in PhCCW, respectively. The characters of A, M and N indicate the inflections points of bands. (d) the measured transmission spectrum of PhCCWs with length $L=200 \mu\text{m}$. In this case, the structural parameters are designed to be the same as that used in (c).

By adjusting the structural parameters mentioned above, we can easily obtain an S-shaped-like coupled defect band with clear inflection points. Figures 1(b) and 1(c) are the two examples of theoretical band structure for the guided modes, which were calculated by the 2D plane wave expansion method with effective index approximation. In Fig. 1(b), there are two inflection points, M and N, with a negatively sloped region in between. By optimizing the design parameters, we were able to obtain a nearly flat region between the two inflection points. In this case, with the band structure shown in Fig. 1(c), both the first derivative and the second derivative of the $\omega(k)$ curve approach zero at the inflection point A. So we have a situation that not only the group velocity of the waveguide mode is very small, but the dispersion of the propagating optical pulse is minimized.

3. Spectral domain measurement

In order to investigate the characteristic of PhCCWs with such special defect bands in the experiments, some design rules are considered here. The input and the output of the PhCCW were integrated with two optical multimode interference (1×2 MMI) couplers for efficient coupling to the outside world [see insert of Fig. 1(a)]. These MMI's, with 50/50 split ratio, allow us to excite and collect the coupled-defect modes at the input and the output ports of the

PhCCW. The interface between the PhCCW and the access strip Si waveguides of the MMI's was properly designed to enhance the coupling efficiency in the slow light region [15]. The width of the waveguides between the PhCCW and the MMI was tapered to ensure single mode propagation in the two branches. PhCCWs with three different lengths ($L = 100, 200$ and $500 \mu\text{m}$) were prepared.

A typical transmission spectrum of the fabricated PhCCW with $200\mu\text{m}$ long is shown in Fig. 1(d). In this case, the structural parameters were designed to be the same as that used in Fig. 1(c). A sharp dip (marked as point "A") can be clearly seen at around $\lambda=1537 \text{ nm}$ indicating that the propagating light suffers a severe change in velocity. Usually for PhC waveguides, the so called "slow light" phenomenon is observed when waveguide modes propagate near the band edge [6]. But here, the dip (or slow light) is in the middle of the transmission spectrum. This is due to the special slow light region associated with the inflection point of the S-shaped-like dispersion relationship caused by the PhCCW.

For further clarification of the S-shaped-like band in PhCCWs, we also investigated the spectral dependence of the group velocities by utilizing interference method. Figure 2(a) shows the schematic of the device layout. An integrated MZI structure [8], which consisted of a reference branch (stripe Si waveguide) and a signal branch (PhCCW butt-connected to MMIs), was used. Two MMI splitters that split light equally between the branches were applied to realize the interference experiments. The structural parameters of PhCCW were designed with the band structure shown in Fig. 1(c).

A typical transmission spectrum of this MZI device is shown in Fig. 2(b). The maximum and minimum of the oscillating fringes correspond to the constructive and destructive interference, respectively. It is seen very clearly that the oscillation period changes rapidly between wavelengths of 1530 nm and 1540 nm . This indicates a sharp increase of the relative phase shift in interference. The group index of the propagating light in the PhCCW can be deduced from this interference spectrum using

$$n_g^{sig}(\lambda) = \frac{\lambda_{min} * \lambda_{max}}{2L(\lambda_{min} - \lambda_{max})} + n_{si}(\lambda)$$

where $L=200 \mu\text{m}$ is the length of a PhCCW and $n_{si}(\lambda)=3.4$ is the index of Si waveguide in the reference branch [8]. Figure 2(c) shows the deduced group index as a function of wavelength. We can see that the group index n_g increases rapidly as the wavelength increases above 1535 nm and reaches the highest value at around 1537 nm , and then diminishes beyond 1540 nm . For comparison, we have also calculated the group index from the S-shaped-like band structure shown in Fig. 1(c) using $n_g = c/(d\omega/dk)$. The result is shown by the black dashed curve in Fig. 2(c). Very good agreement was obtained between the measured and the calculated results, demonstrating the existence of small group velocities at around $\lambda=1537 \text{ nm}$, which corresponds to the inflection point, "A", shown in Fig. 1(c) and the dip shown in Fig. 1(d).

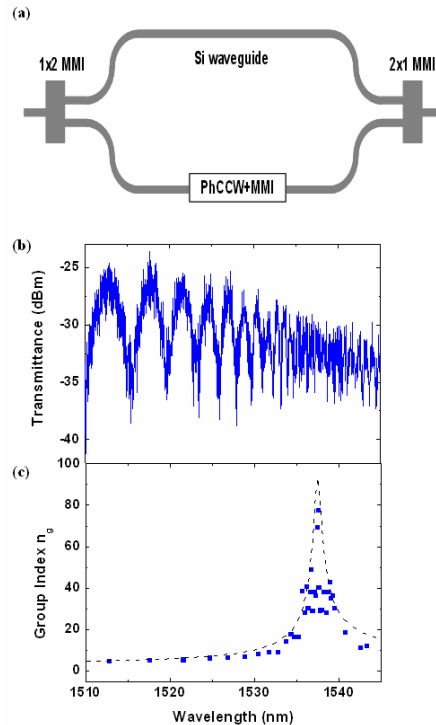


Fig. 2. (a). Schematic of an integrated MZI structure. The gray bold line represents the stripe Si waveguides. (b) Measured transmission spectrum of a MZI sample. In this case, the length and the lattice constant of PhCCW are 200 μm and 438 nm, respectively. (c) Wavelength dependence of group indices (blue squares) deduced from (b) by using inference approach. The black dash line shows the theoretical group indices calculated from the inverse of slopes of the blue line (coupled band) in Fig. 1(c).

4. Time domain measurement

Next, we explore the temporal dynamics of the propagating light in this special slow light region by doing the time-resolved measurements on the PhCCW. A passive mode-locked Er-doped fiber ring laser, operated in the 1525-1565 nm range, was used as the light source. Optical pulses with width of 24-28 ps (FWHM) and a repetition rate of 10 MHz were used for the measurement. The input signal was steered into two paths by an optical splitter. One went to the PhCCW which we wanted to test and the other went into an optical delay line. The signals were then combined at the output and the waveform was displayed and recorded by a high speed oscilloscope, which, with a fast integrated optical-module, had a 28 GHz of unfiltered optical bandwidth for optical signal detection.

In order to determine the group velocity of the waveguide mode, we used PhCCWs with three different lengths ($L=100, 200, \text{ and } 500 \mu\text{m}$). Since the optical delay line was the same for all three samples, the transmitted pulse from the delay line was used as a reference and the waveforms measured from samples with different lengths could be overlapped to show the propagation delay in the PhCCWs. Figures 3(a)-3(c) show the transmitted pulses through the PhCCWs and the optical delay line recorded on the oscilloscope. (a), (b), and (c) correspond to measurements with input pulses of three different wavelengths $\lambda = 1541.02 \text{ nm}, 1539.38 \text{ nm}$ and 1537.30 nm , respectively. The reference signal is the left most pulse in each figure and other pulses are measured waveforms of the transmitted light from the three samples. By measuring the delays of the output pulses with respect to the reference signal, the group velocity was then determined. Take Fig. 3(b) as an example, the duration time between the output pulses and the reference pulse was 99, 108, and 132 ps for samples with length $L = 100, 200 \text{ and } 500 \mu\text{m}$, respectively. Plotting the duration time versus the waveguide length

and fitting the data with a linear line, [see Fig. 3(d)] we obtained a group velocity of $0.039c$. Similarly, the group velocity determined from the curves in Fig. 3(a), where the input pulse has a center wavelength of 1541.02 nm, is $0.050c$.

In Fig. 3(c), where the input pulses have a center wavelength of 1537.30 nm, the pulses clearly travel slower than those in the other two cases. The output waveform for the sample with $L=500\ \mu\text{m}$ is very weak. But if we magnify the picture, a clear output waveform centered at $t = 430\ \text{ps}$ can be seen [see Fig. 3(e)]. From the delay time measured in Fig. 3(c), we

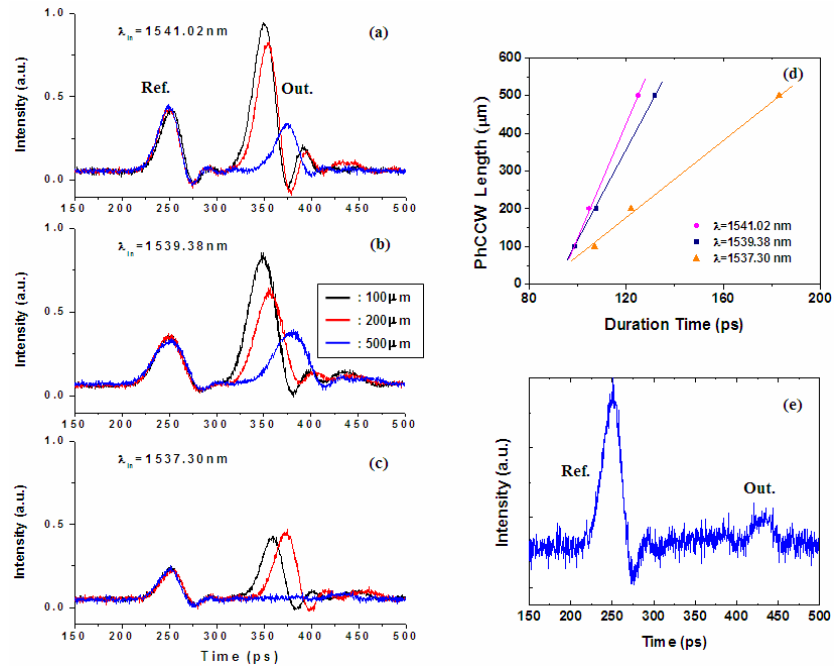


Fig. 3. Time-resolved measurements obtained by recording output pulses on the oscilloscope. The black, red, and blue lines represent samples with PhCCW length of $L=100$, 200 , and $500\ \mu\text{m}$, respectively. The waveforms in the leftmost of plots, named reference signals (Ref.). Others correspond to output signals (Out.), which means pulses travel through PhCCW.

Measurements at different central wavelengths of launched pulses $\lambda = 1541.02\ \text{nm}$, $1539.38\ \text{nm}$, and $1537.30\ \text{nm}$ are shown in (a), (b), and (c), respectively. The magnified plot of the blue line in (c) is shown in (e). A weak output signal is clearly observed. (d) The measured duration time with different launched wavelengths as a function of PhCCW length.

determined a very slow group velocity of only $0.017c$. In other words, the speed of light is slowed down by about sixty times than that in vacuum.

Using the same method, we have investigated the frequency dependence of group velocity in the wavelength range from $1545.00\ \text{nm}$ to $1537.30\ \text{nm}$ and compared it with the theoretically calculated group velocities obtained from the slopes ($d\omega/dk$) of the band structure in Fig. 1(c). The result is shown in Fig. 4(a). The deviation between the measured points and the theoretical curve is due to fabrication disorder, which results in slight difference in structural parameters. In spite of this discrepancy, it clearly shows that the group velocity goes down as the launched frequency approaches the inflection-point “A”. These extremely small group velocities are attributed to a relatively flat region in the band structure of the coupled waveguide modes. The slow light region is in the middle of the transmission spectrum of the waveguide mode. This is different from the previously reported slow light experiments in single line-defect PhC waveguides, where the waveguide modes propagate near the zone edge (or the edge of the transmission spectrum) of the band structure. This gives us a larger tolerance in obtaining the slow light region.

From the curve shown in Fig. 4(a), we can evaluate the value of group velocity dispersion (GVD) defined as $-(dv_g^{-1}/d\omega)$. Fig. 4(b) shows the calculated GVD (black line) and the experimentally obtained GVD (blue line), which is obtained after curve fitting the data points in Fig. 4(a). Despite the offset in frequency in Fig. 4(b), a good qualitative agreement between the two was obtained. Different from those of the W1 type PhC waveguides [11, 12], the calculated dispersion curve has a positive and a negative part, and in a very narrow region in between it goes to zero. Therefore, it is possible that by reaching the center point “A” one may obtain an extremely small group velocity with zero dispersion. Due to the narrow bandwidth of this reduced GVD region in the current design and the limitation of the measurement system, however, we did not succeed in exploring such reduced GVD region in the experiment. We believe that by further optimizing the PhCCW structure to enlarge the bandwidth of the low dispersion region [13] or by launching a longer pulse length, it is possible to observe that the guided modes propagate along the PhCCW at an extremely group velocity and minimized dispersion.

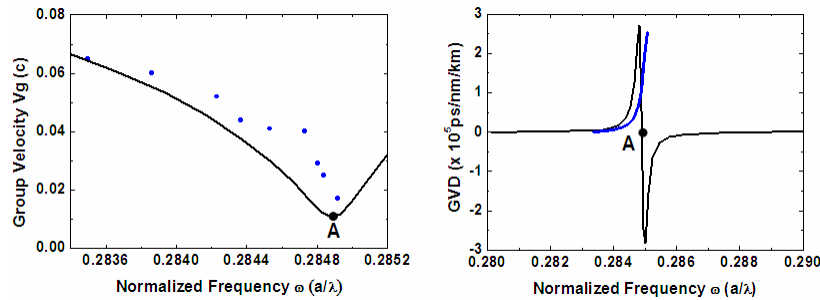


Fig. 4. (a). Measured group velocities (blue dot) in comparison with theoretical ones (black line), which are derived from the calculated band diagrams in Fig. 1(c). The character “A” indicates the calculated inflection point of the coupled bands. The lowest group velocity in experiments is about $0.017c$ at $\omega=0.2849$ (or $\lambda = 1537.30$ nm). (b) Calculated GVD (black line) from Fig. 1(c) and experimental GVD (blue line) derived from measured V_g in Fig. 4(a).

5. Conclusion

We have designed and fabricated a photonic crystal coupled waveguide, where the guided mode has a unique flat band region within its photonic band gap allowing slow light propagation. Special inflection-point slow light modes that appear in the middle of the transmission spectrum instead of at the band edge were obtained. A sharp dip in the transmission spectrum and the peaking of the group index from the Mach-Zehnder interference measurement clearly indicate the existence of such inflection point. The group velocities of the optical pulses in this special waveguide were measured in time domain by comparing the propagation delay of the optical pulse through the waveguide with that of a reference optical delay line. A very clear slowdown of the optical pulses was directly recorded on a fast oscilloscope. An extremely small group velocity of $0.017c$ has been observed at $\lambda=1537.30$ nm, due to the inflection-point slow light modes. This study, to our knowledge, is also the first consistent and reliable observation of the inflection-point slow light in the spectral and time-domain analysis.

Acknowledgments

The authors wish to thank Dr. Shinya, Dr. Tanabe, and Dr. Taniyama in NTT for their fruitful suggestion about the device design and experiments. S.C. Huang acknowledges the financial support provided by National Science Council of Taiwan and NTT Basic Research Laboratories of Japan.